

MISSION ANALYSIS FOR A POTENTIAL MARS SAMPLE RETURN CAMPAIGN IN THE 2020'S

Austin K. Nicholas*, Alan Didion†, Frank Laipert‡,

Zubin Olikara§, Ryan C. Woolley**, Rob Lock††, Jakob Huesing‡‡

The Mars 2020 mission, currently under development by NASA, plans to acquire and cache carefully-selected rock and regolith samples from the surface of Mars for potential future return. NASA and ESA are jointly studying options for returning those samples to Earth with missions launching in the 2020s. This paper demonstrates a method for modeling the various campaign elements, synthesizing coordinated campaign timelines, and assuring trajectory feasibility in the presence of many constraints, and finally optimizing towards mission success. Options for complete sample return campaigns in multiple launch and arrival opportunities are explored and compared.

INTRODUCTION

National Aeronautics and Space Administration (NASA) and the European Space Agency (ESA) have announced plans to study potential Mars sample return (MSR) campaigns to retrieve samples to be emplaced by Mars 2020¹. The notional campaign includes three flight elements:

- The Mars 2020 rover (M2020), to find and collect scientifically compelling samples
- A Sample Retrieval Lander (SRL)², to retrieve the samples and launch them into orbit. The SRL includes:
 - A Sample Fetch Rover (SFR), to drive to the samples and bring them back to the SRL
 - A Mars Ascent Vehicle (MAV), to launch the samples into orbit

* Systems Engineer, Project Systems Engineering and Formulation

† Systems Engineer, Project Systems Engineering and Formulation

‡ Mission Design Engineer, Flight Path Control

§ Mission Design Engineer, Inner-Planets Mission Analysis

** Mission Design Engineer, Inner-Planets Mission Analysis

†† Manager, Mars Program Formulation Office

(All Above Authors): NASA Jet Propulsion Laboratory, California Institute of Technology, 4800 Oak Grove Drive, Pasadena, CA 91109.

‡‡ Systems Engineer, Systems and Concurrent Engineering Section, European Space Agency, European Space Research & Technology Centre, Keplerlaan 1, 2200AG Noordwijk, The Netherlands

- An Orbiting Sample container (OS), which holds the sample tubes during the MAV ascent, on-orbit planetary protection activities, and through Earth return
- An Earth Return Orbiter (ERO)³, to capture the samples and return them to earth in an Earth Entry Vehicle (EEV)

This paper is submitted as part of a group of papers that each discuss some of the recent work that shapes the architectural opportunities and feasibility analysis leading to the specific architecture options in the current study. The papers submitted with this one are based on the architecture options described in this paper. These papers are:

- Woolley, et al, “Low-Thrust Trajectory Bacon Plots for Mars Mission Design,”⁴ describes low-thrust analogs to pork chop plots for Mars missions including the MSR campaign architecture studies. These bacon plots underlie the end-to-end mission analysis for all of the architectures in the current MSR studies.
- Laipert, et al, “Hybrid Chemical-Electric Trajectories for a Mars Sample Return Orbiter,”⁵ defines methods for developing trajectories for Mars sample return orbiters using both solar electric propulsion and high impulse chemical propulsion systems.
- Haw, et al, “Mars Sample Return - Orbital Rendezvous Detection Methods,”⁶ describes key navigation trade studies for detection of the orbiting samples at Mars that have strong influence on the architecture of the Sample Return Orbiter.
- Olikara, et al, “Chemical and Solar Electric Propulsion Orbit Matching for Mars Sample Rendezvous,”⁷ describing orbit matching concepts for time efficient rendezvous with orbiting samples at Mars for sample return orbiters using chemical propulsion or electric propulsion.
- Nicholas, et al, “Simultaneous Optimization of Spacecraft and Trajectory Design for Interplanetary Missions Utilizing Solar Electric Propulsion,”⁸ in which a tool (“MORT”) is described for simultaneously optimizing the spacecraft design alongside the trajectory given mission constraints and objectives. MORT is essential for primary parameter exploration, first order spacecraft sizing and mission timeline assessment for MSR mission architecture development.
- Lock, et al, “Potential Campaign Architectures and Mission Design Challenges for Near-Term International Mars Sample Return Mission Concepts”⁹ discusses the motivation, previous work, and current study efforts surrounding Mars Sample Return. This includes an architectural description of the current missions under study, their major roles, foreseen implementation, and future trades being considered.

More details about the overall architecture can be found in the companion paper by Lock⁹. This paper focuses on the process for assembling the mission concept design for the SRL and ERO at the campaign level to ensure campaign feasibility.

PROBLEM DESCRIPTION

This section contains a brief description of the relevant SRL and ERO activities, the mission opportunities under consideration, and the main challenges to be addressed.

The analysis in this paper was performed by JPL for the purpose of campaign-level architecting. Having all the models in one place allows for rapid exploration of large architecture spaces and searches for global campaign optima in the early development phase. This is also necessary because both ERO and SFR are currently undergoing competitive industry studies, limiting the amount of information which can be released. Where possible, for the ESA-provided elements (ERO and SFR), effort was made to coordinate models with ESA to ensure representativeness

alongside on-going ESA assessments, but these do not represent ESA or NASA commitments or final designs. As a result, information on the spacecraft designs (e.g. equipment lists, subsystem choices) will be kept to very high level in this paper.

SRL Mission Concept Scenario, Assumptions, and Constraints

The SRL is currently envisioned to have the following primary activities:

- **Launch.** The mission begins with launch from Earth. The SRL is anticipated to be launched on a US launch vehicle commercially available in the mid-2020's, from Cape Canaveral. Launch declinations above 28.5° are penalized. For the purpose of analysis in this paper, the mass lift capability of Atlas V 551 is used as a constraint, which should also ensure compatibility with other launch vehicles such as Vulcan, Falcon Heavy, New Glenn, and OmegA which may be available in this timeframe.
- **Cruise.** After launch, the SRL travels from Earth to Mars, doing trajectory correction maneuvers as necessary to target the entry interface. SRL is currently envisioned to strongly leverage the MSL and M2020 cruise stage design. Because these cruise stage designs have very limited propellant, a nearly-ballistic transfer would need to be chosen.
- **EDL.** Upon arrival at Mars, the cruise stage would be jettisoned and the SRL sheds its velocity rapidly using its aeroshell, parachute, and propulsive landing system. It is also assumed that SRL would draw heavily on the design of the M2020 EDL design, which imposes constraints on entry velocity, to be kept below around 6.1 km/s inertial. Like M2020, SRL is envisioned to use Terrain Relative Navigation (TRN) to improve landing safety in order to land near the M2020 landing site in Jezero crater. TRN matches images taken during EDL to orbital images to determine the SRL position and then divert to a safer location. Because TRN is image-based, this imposes a solar elevation angle constraint of at least 20° with 30° - 50° being ideal.
- **Deployment and Checkout.** After landing, the SRL performs deployments and system checkouts. This is expected to take up to 5 sols.
- **Sample Retrieval.** The SRL deploys the SFR, which would traverse up to 20 km to the depot location(s) established by M2020, acquire the sample tubes, and return them to SRL. The length of this phase varies strongly based on landing location and SFR system design. This will be addressed in more detail later. M2020 may also deliver some samples directly to the SRL.
- **Sample Transfer and Loading.** The SRL uses its robotic arm to transfer the samples from the SFR to the OS. This is expected to take up to 20 sols.
- **Prepare for MAV Launch.** Once all samples are transferred, the MAV must be configured for launch, heated to its operational temperature and calibrated for launch. It is assumed that the ERO should be on-station during these activities to ensure the proper orbit can be targeted. This is expected to take around 10 sols.
- **MAV Launch.** The MAV engines ignite and it is guided into its final orbit, where the OS is released. The SRL and/or SFR missions may continue after this point, but there is no longer any impact on MSR. This phase includes up to 14 sols to enable multiple launch attempts.

The primary open variables in terms of campaign optimization for SRL are:

- The launch and EDL date (based on the trajectory design and launch feasibility)
- Landing precision (currently assuming M2020-like capability, but other enhancements to improve accuracy may be needed).
- Power and thermal system design. No decision has been made on the power or thermal system design of SRL or SFR. Per programmatic guidance from NASA, the baseline design for each is solar power only, but engineering issues could spur consideration of radioisotope systems.
- The SFR drive speed and autonomy needed to meet its available timeline

The surface mission is strongly affected by the Mars surface environment. Throughout this paper, these will be referenced using solar longitude (“Ls”). Ls=0 corresponds to northern hemisphere spring equinox, Ls=90 is northern summer solstice, and so on.

ERO Mission Concept Scenario, Assumptions, and Constraints

The ERO is currently envisioned to have the following primary activities:

- Launch. The mission begins with launch from Earth. The ERO is assumed to launch on an Ariane 6.4 from Kourou, which imposes significant penalties for launch declinations above around 5 degrees.
- Outbound Transfer. After launch, the orbiter travels from Earth to Mars. For Electrical Propulsion (EP) options, it will be primarily thrusting in this phase.
- Mars Orbit Insertion (MOI). Upon arrival at Mars, a large orbit insertion maneuver is performed using the Chemical Propulsion (CP) system (not present in all-EP options).
- Altitude Lowering. Uses a combination of CP and/or EP and/or aerobraking to reduce altitude to Low Mars Orbit (LMO).
- Low Mars Orbit. In this orbit, the ERO supports the SRL with relay communications, observes the MAV launch, and performs rendezvous and capture with the OS. Of particular importance is the orbit-matching phase, which is addressed in more detail in the companion paper⁷.
- Altitude Raising. Uses a combination of CP and/or EP to increase altitude for Mars departure.
- Trans-Earth Injection (TEI). A large maneuver used to escape Mars orbit (not present for all-EP return options).
- Inbound Transfer. The orbiter returns to Earth. For EP options, it will be primarily thrusting in this phase.
- Earth Arrival. Upon arrival at Earth, the orbiter separates from the Earth Entry Vehicle (EEV) containing the samples. The EEV enters the atmosphere while the orbiter performs an avoidance maneuver to avoid entry. It is assumed that the EEV could support entry speeds as high as 13 km/s inertial, but speeds of 12 km/s or lower would be preferred.

A primary issue to be addressed in this paper is the choice of propulsion architecture. Two main types of propulsion are considered: CP (assumed to be a 1 kN-class bipropellant engine of ~320s Isp) and EP (multiple engine options considered). Hybrid (Hb) options utilize both propulsion types in an optimal way for a given leg. A hybrid outbound utilizes EP during the heliocen-

tric phase, uses the CP system for MOI (and optionally some apoapsis reduction), and then completes the transfer to LMO using EP. A hybrid inbound utilizes EP to raise orbit, CP for final altitude raising and TEI, and then uses EP during the heliocentric phase. More information on hybrid transfers can be found in the companion paper⁵. Because hybrid missions typically want large, mass-efficient solar arrays to power the EP systems, it is assumed that these arrays are not compatible with aerobraking.

Early in the study it was determined that a two-stage vehicle would be necessary to meet mass and timeline constraints. The initial assumption for the place to perform the staging is in Mars orbit, after rendezvous. This is because many of the functions of the ERO are no longer needed after the MAV is launched and the OS is captured (relay and high-data telecom, OS detection, OS capture), and associated hardware could be jettisoned in addition to propulsion components. Some variation on this is possible (for example dropping the CP stage from the Hb-EP architecture after MOI), but these effects are expected to be second-order compared to the overall propulsion architecture choice, and in this work the staging is modeled as occurring after OS capture and before altitude raising. Figure 1 shows the options considered, with the major impulsive maneuvers shown in brackets. Certain cases are listed as “degenerate” because if these architectures are optimal, they would show up in the results as variants of other architectures with special characteristics. For instance, an EP-Hb option would show up as a Hb-Hb option utilizing no CP propellant on the outbound leg. This is useful to reduce the number of cases to be simulated without actually losing any options.

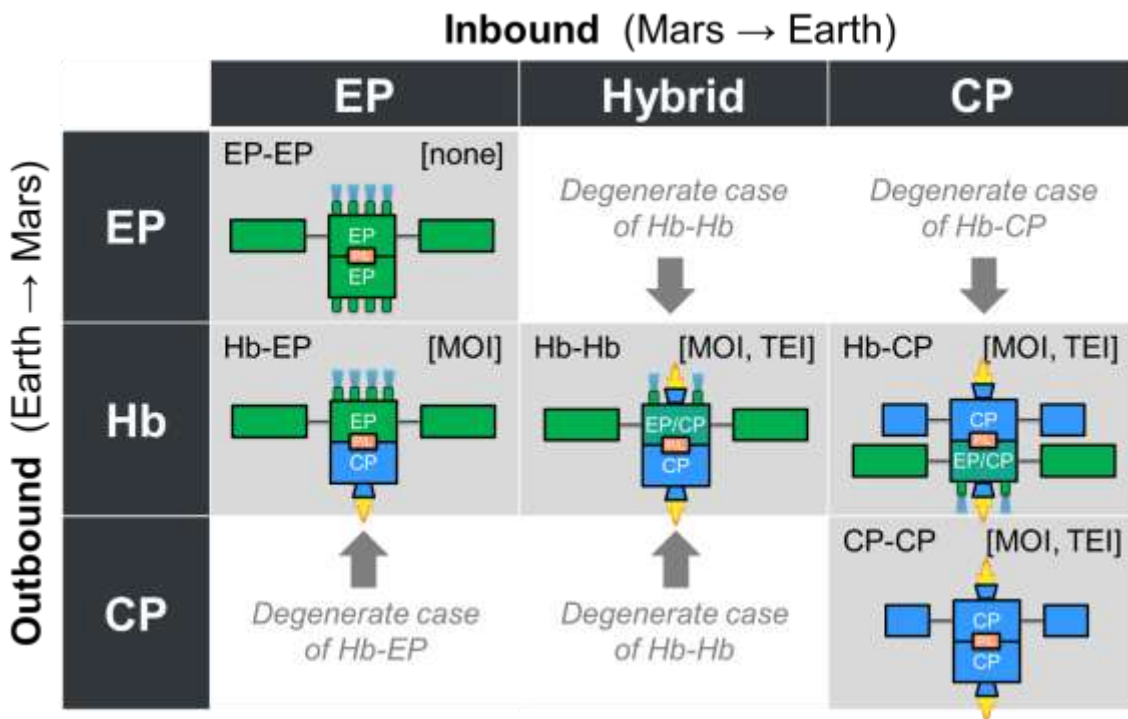


Figure 1. Summary of ERO Propulsion Architecture Options

For the EP-involving options, several EP engines were considered, as it is a key propulsion trade and critical to the ultimate feasibility of these options. Because the ERO is a European mission, engines available in Europe were considered and are listed in Table 1. Table values are given at maximum power for context; performance curves as a function of available power are used

in the analysis. Lastly, it is worth noting that these values are used for analysis purposes and may differ somewhat from the exact capabilities of the systems.

Table 1. EP Thrusters Analyzed

Thruster Name	Developer	Code	Power [kW]	Thrust [mN]	Isp [s]	Thrust / Power [mN/kW]	String Mass [kg]
T6	QinetiQ	T6	5.0	145	3894	29	51
RIT 2X	Ariane Group	RIT	6.3	190	3872	30	77
PPS5000	Safran	PPS	5.5	292	1750	53	41

The primary open variables in terms of campaign optimization for ERO are:

- Earth Launch, Mars Arrival, Mars Departure, and Earth Arrival dates.
- Earth launch vehicle C3 (and associated mass limit)
- Propulsion architecture and component choice
 - For EP-involving options, the EP engine technology and array size
 - For hybrid options, the mix of CP / EP maneuver types and resulting trajectories
 - For CP-only options, the aerobraking strategy and sizing of drag flaps
- Staging strategy (All options stage some propulsion, but the staging of other equipment such as parts of the payload, antennas, cameras, and reaction wheels, may be used to improve launch vehicle margin or reduce transfer times)
- Capture, Containment and Return System (CCRS) payload mass and EEV entry speed.
- The timeline used for rendezvous and capture activities

Additional Campaign-Level Considerations

Aside from the SRL and ERO mission-level issues mentioned previously, there are a few other relevant issues to be considered at the campaign level (e.g. between different missions).

The first and most important consideration is the potential interaction of the ERO and SRL missions in-flight. For this study, it is assumed that the ERO must be present at the time of MAV launch to provide relay coverage and so that it can be on-station to perform optical detections of the OS and determine its orbit for rendezvous. Based on analysis of the rendezvous phase, it is assumed that an absolute minimum of 2 months in LMO is needed to accomplish MAV launch and rendezvous objectives, with more time (up to 5 months total) being strongly beneficial. In contingency cases, the OS can still be located optically if the ERO is not on station for MAV launch, but the search process is much faster if the observations are taken immediately after MAV launch.

The next issue is relay communication support for SRL¹⁰. The ERO would be equipped with UHF communication equipment similar to MAVEN or TGO, but in some cases, it may be beneficial for SRL to arrive at Mars before ERO is in place to support it. It is assumed that existing assets (MRO, MAVEN, or TGO) would provide relay support. However, these orbiters will be well past their prime mission and design lifetime by the late-2020's.

The last consideration is the use of M2020 for sample delivery to SRL. The feasibility of such an approach has been studied and the technical solution for transferring tubes from M2020 to

SRL is of minimal impact to the solution already needed for transferring tubes from SFR. Therefore, it is considered that SRL would be compatible with deliveries from both vehicles, perhaps delivering different sets of the sample tubes. Like the orbital missions, M2020 will be beyond its prime mission in this time period.

Summary of Main Challenges

There are a multitude of constraints and objectives to be considered, but the most important are:

- SRL Delivery Trajectory Feasibility – does the spacecraft mass, including propellant for maneuvers, fit within the assumed launch vehicle capability and boundary conditions on entry delivery?
- SRL Surface Mission Feasibility – is the time on the Mars surface between SRL landing and MAV launch sufficient to complete the surface mission?
- ERO Trajectory Feasibility – does the spacecraft mass, including propellant for maneuvers fit within assumed launch vehicle capability and match timeline constraints?
- ERO On-Orbit Timeline Feasibility – is the time in Mars orbit between MAV launch and Mars Orbit departure sufficient to find the OS, capture it, and prepare for return?
- SRL-ERO In-Flight Interaction and Timing – are SRL and ERO in the right places at the right times to make the needed operations work?

A feasible campaign must satisfy all of these constraints, preferably with as few risks and new technologies as possible, while maximizing the chance of mission success.

Summary of Campaign Opportunities

Due to programmatic and development constraints, both SRL and ERO are constrained to launch in mid-2026, at the earliest. Fortunately, there is a good Earth-Mars transfer window in late-2026. The next opportunity is around 2 years later, in late 2028. This opportunity is also considered. For 2028 launch opportunities, a 2027 launch with a one-year Earth gravity assist is also possible and sometimes helpful. This is still grouped into the “2028” opportunity because those options all have similar Earth-Mars transfers. Return opportunities also follow a 2 year cycle, with opportunities in late 2029, 2031, and 2033.

Table 2 shows all of the launch and return options which include launches in the 2020’s. The nomenclature “26/26/29” means SRL launched in 2026, ERO launched in 2026, samples returned to earth in 2029. For the purpose of this paper, two characteristic families will receive analytical focus. The first is the “fast return” or “3 year” family of 26/26/29 and 28/28/31. This family gets to Mars quickly and returns in the next launch window. The second is the “5 year” family of 26/28/31 and 28/28/33. The mixed families of 28/26/31 and 26/28/31 are not described in detail but are bounded by the 3 year and 5 year families. If these options emerge as programmatically interesting in the future they would be studied in more detail. In the remainder of the paper, the 26/26/29 and 26/26/31 options will be studied in depth and with comments on the other opportunities at the end.

Table 2. Launch and Return opportunities summary. Nomenclature for campaign year abbreviations is: [SRL Launch] / [ERO Launch] / [ERO Return]

	2026 SRL		2028 SRL	
Return Date	2026 ERO	2028 ERO	2026 ERO	2028 ERO
2029	26/26/29	Impossible	Impossible	Impossible
2031	26/26/31	26/28/31 (between 26/26/31 and 28/28/31)	28/26/31 (between 26/26/31 and 28/28/31)	28/28/31 (mostly similar to 26/26/29)
2033	(minimal benefit vs 26/26/31)	(minimal benefit vs 28/28/33)	(minimal benefit vs 28/28/33)	28/28/33 (mostly similar to 26/26/31)

26 / 26 / 29 CAMPAIGN OPTION

The 26/26/29 (3-year) option is studied first. From a timeline perspective, it is clearly the most challenging option and speed is critical in every phase of the mission.

SRL Trajectory

For a 3-year campaign, it is desired that the SRL arrive as early as possible within the relevant constraints. The typical ballistic half-revolution (type I/II) transfers with direct entry are used. Figure 2 shows the porkchop plot for this transfer type. The chosen launch period is a type II and is shown in magenta. This launch period was selected as a balance of early arrival, launch energy, entry velocity, and lighting angle. The type I options, although arriving earlier, do not have sufficient lighting angle for TRN and have higher entry speeds, and therefore cannot be used. The primary output of this process is the arrival date of July 27, 2027 at $L_s=137$. It should be noted that this is a representative launch period only and that this does not represent a fully refined design. Small changes (e.g. moving the arrival date earlier or later by a few days) can be expected, but should not majorly affect the analysis at this high level. If the launch vehicle constraint were relaxed significantly (e.g. by moving to a heavy launcher), the SRL would still not be able to arrive more than about one month earlier (around July 1, 2027 at $L_s=124$) due to the lighting constraint.

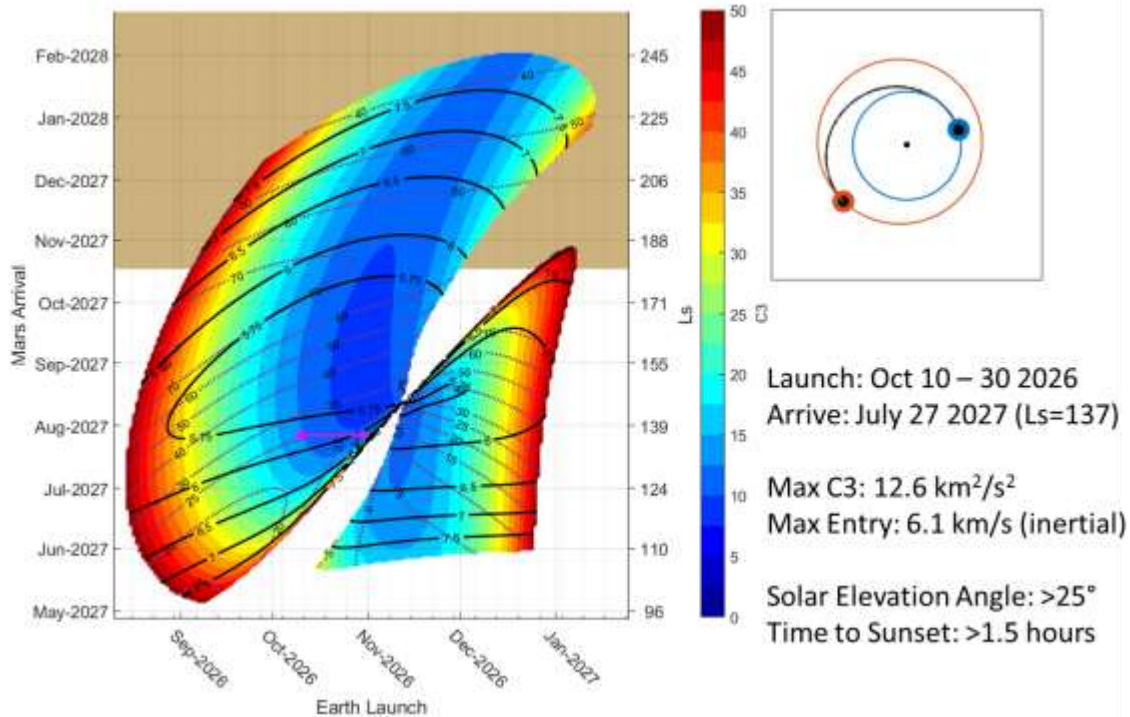


Figure 2. SRL launch/arrival options (“porkchop plot”) for 26/26/29. Colored contours are launch energy (C3) in km^2/s^2 , solid black contours are inertial entry speed, in km/s , dotted purple contours are the solar elevation angle at landing, in degrees. The tan region corresponds to $L_s=180$ to 360 and denotes the time when global dust storms are most likely. The magenta line is the selected launch period. An illustration of the trajectory and some figures of merit are shown on the right.

ERO Trajectory Options

The ERO trajectory options are far more complex than the SRL due to the additional maneuvers (altitude lowering, maneuvers in LMO, and the return leg) as well as the myriad propulsion options available both in terms of type (CP vs EP vs Hybrid), sub-options within each family (engine type, subsystem sizing, etc) as well as other system parameters such as staging and payload mass. When considered fully, this is an extremely large amount of options, with no clear way of making initial reduction in the tradespace. Especially in the presence of the strong timeline constraint associated with 26/26/29, mass-based intuition is not always correct.

Example CP and hybrid outbound transfer options from Earth to LMO are shown in Figure 3. Note that the CP option is not the same as the usual porkchop plot because it also includes the time needed for aerobraking. For each point in the plot, the heliocentric transfer and planetocentric transfers are jointly optimized to maximize the LMO delivered mass for the given launch and arrival date constraints. In both cases, delaying the LMO arrival allows a more efficient transfer by improving the heliocentric transfer and/or reducing the amount of apoapsis reduction needed using CP and instead using aerobraking (CP case) or EP (hybrid case). It can be seen that the hybrid cases can deliver approximately 500 kg more mass to LMO, even including the fact that they need to arrive earlier to support an EP-based return. However, hybrids also have higher dry mass due to additional propulsion components.

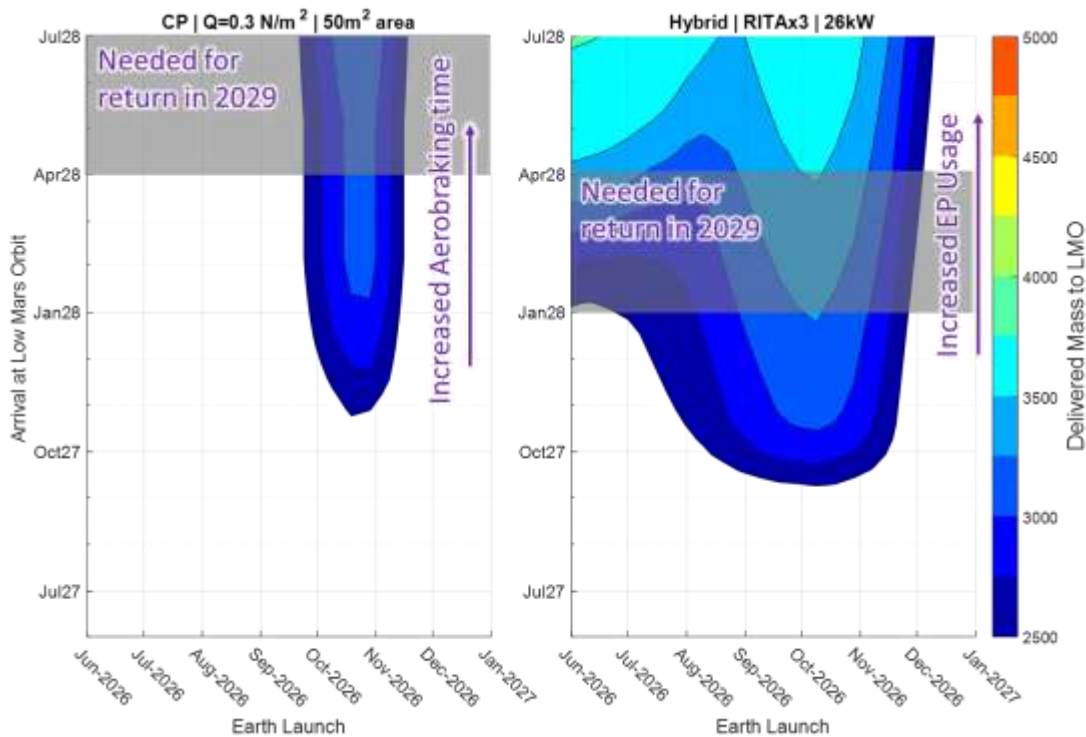


Figure 3. Example Outbound ERO transfer options for 26/26/29 option. Left: CP with aerobraking, Right: Hybrid. Approximate LMO arrival dates consistent with return in 2029 are shown in the gray boxes. Exact arrival date needed in these ranges depends on return trajectory and rendezvous strategy. These plots include a 21 day launch period in each point.

Timeline Modeling at Mars

The time period when one or both missions are at Mars has many steps which must happen (outlined in earlier sections) in order to get the ERO onto its return trajectory. Although some things can happen in parallel, there is essentially one “critical path” starting with the SRL EDL and ending with the completion of ERO payload activities that determines readiness for departure. For each of these activities, a probabilistic model was created to capture the likely time each event would take to complete. For some models (e.g. MAV heating), the activity usually takes around the same amount of time in all cases. In others (e.g. tube loading), the variation is primarily driven by operations and anomaly resolution. For OS optical detection and orbit matching, the time is driven by the MAV launch dispersion, which is probabilistically modeled^{6,7,11}. The SFR surface mission is both the longest consumer of time and the most complicated to model. This is because the traverse distance results from the dispersion of the landing ellipse and can vary from almost none to 20km. Further, SFR is primarily energy-limited, especially in the traverse legs, so the speed is not constant over the mission as its available energy varies with season, atmospheric dust, and dust accumulation on the solar panels. An example of the impact of this is shown in Figure 5.

In addition to the expected events, there is an additional complication arising from environmental effects that could interrupt the timeline. In this case, there are two primary causes: dust storms (affecting only the surface mission) and solar conjunction. Dust storms happen roughly one in three Martian years and are difficult to predict aside from historical evidence showing the large global ones happen primarily between Ls=180 and 360. Conjunction is completely predict-

able based on Earth-Sun-Mars geometry and happens to fall just in the middle of the timeframe of interest, centered in March 2028. When either of these interrupts happen, it is assumed that the timeline is paused. It is further assumed that the MAV launch and orbit matching would not be initiated before conjunction unless rendezvous would be completed prior to conjunction. This introduces a keepout zone for MAV launch of around 2 months before conjunction. Figure 6 shows an example probabilistic result for the readiness of ERO to begin its departure spiral based on these models. The gap around April 2028 is due to solar conjunction.

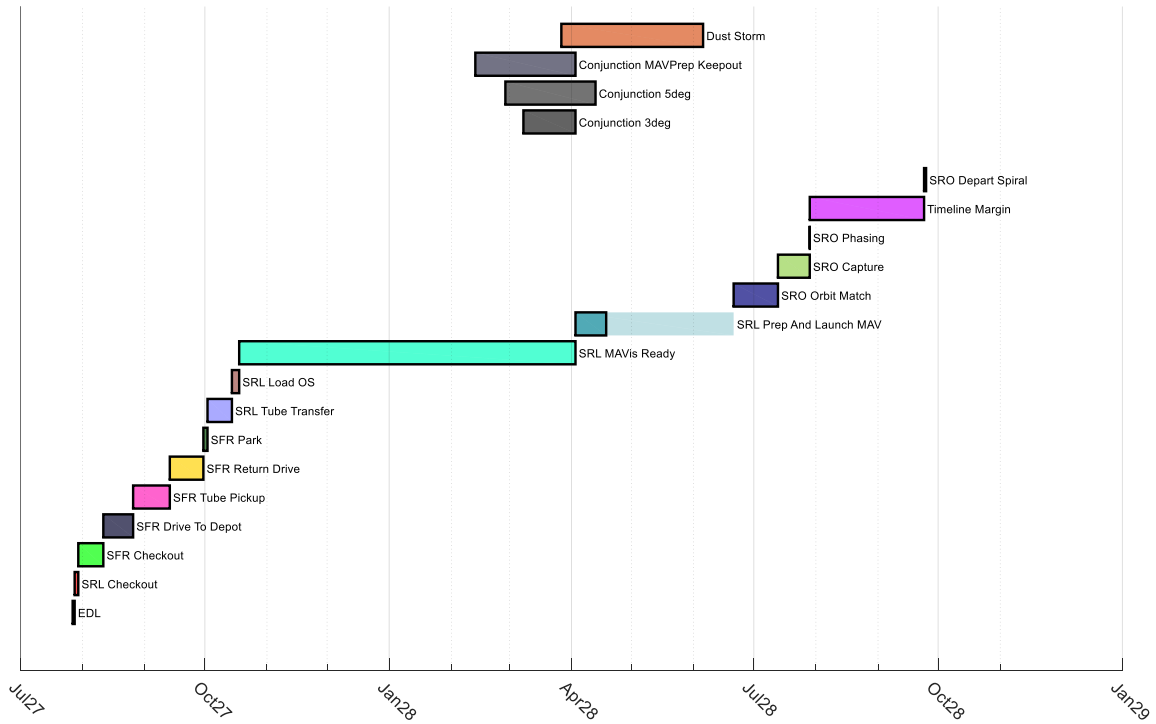


Figure 4. Critical path timeline events at Mars.

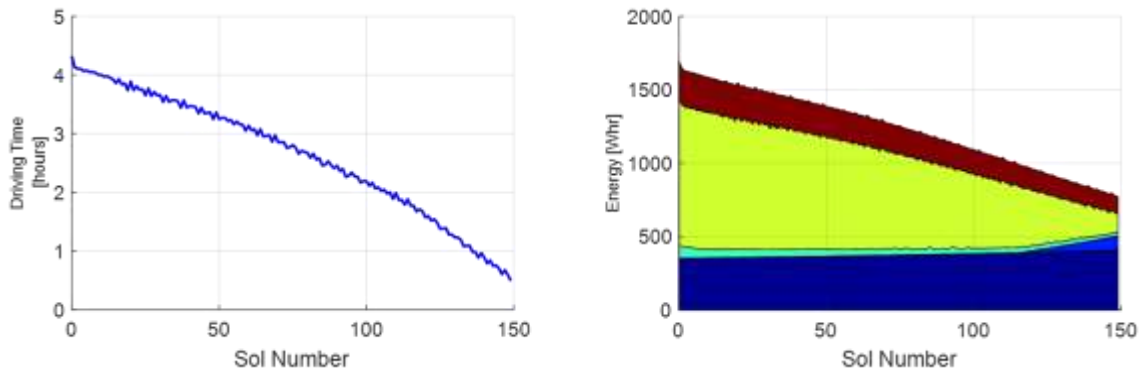


Figure 5. Example MaSMO results for SFR Traverse starting Ls=139. Left plot: drive time per sol. Right plot: energy use each sol. Energy use categories are – dark blue: sleep and communications, light blue: survival heating, teal: actuator heating, yellow: driving, dark red: losses.

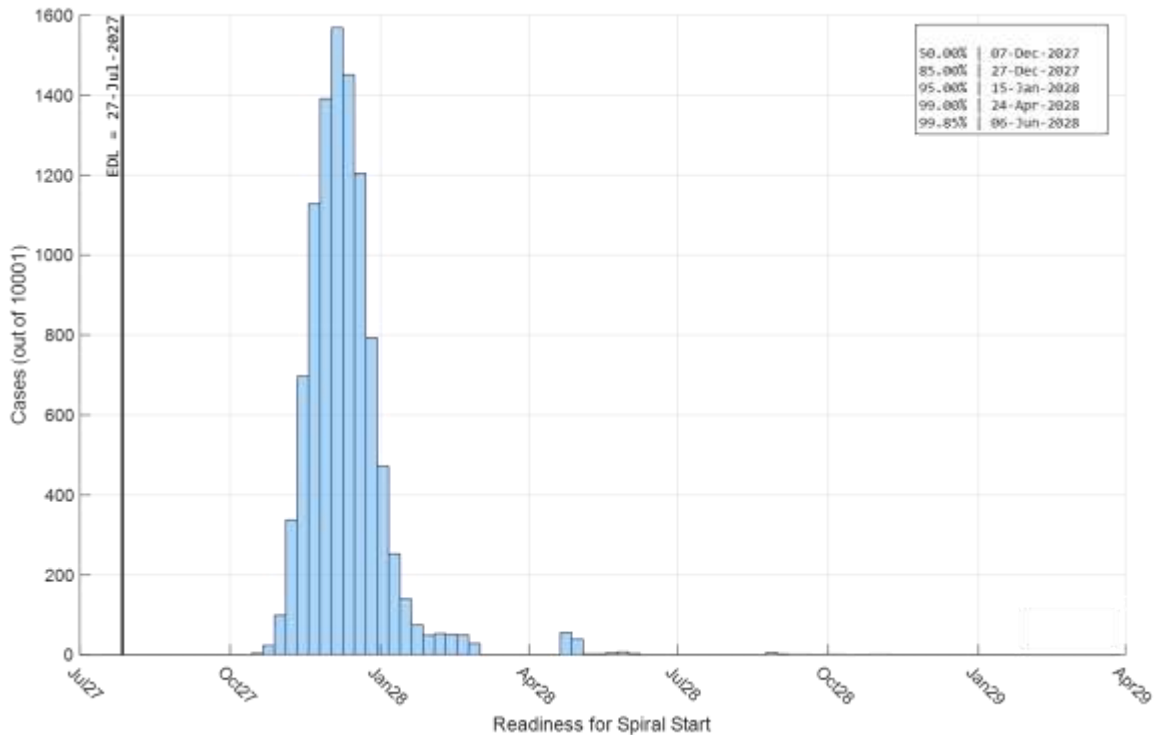


Figure 6. Probabilistic timeline results showing readiness for departure for 10,001 cases

Campaign-Level Optimization

At this point, it becomes clear that more powerful tools than porkchop and bacon plots are needed to really optimize this problem when considering the number of design variables involved. A variety of tools were linked together for this purpose of campaign-level global optimization. These tools are listed below and shown in Figure 7:

- MORT – to support simultaneous optimization of ERO and its trajectory for a variety of subsystem choices and date ranges. For more info on MORT, see the companion paper⁸
- Mars Surface Mission Optimizer (MaSMO) – this tool is used to model the rover performance as a function of energy, atmospheric, and rover system models. Further description of this process would be interesting but is out of scope of this paper.
- Mars 2020 Traversability Tools (MTTT) – this JPL-developed tool^{12,13} predicts rover drive times based on maps of the landing sites and known goal locations
- SRL Porkchops – used to determine SRL trajectory options. For 26/26/29, there is really one “best” result, but in other cases it is less straightforward.
- Probabilistic Campaign Timeline Model (PCTM) – optimization framework for iterating between missions to find a “campaign-optimal” solution for a variety of figures of merit. This tool is the one which would weigh the surface mission timeline against the orbital mission trajectory feasibility.

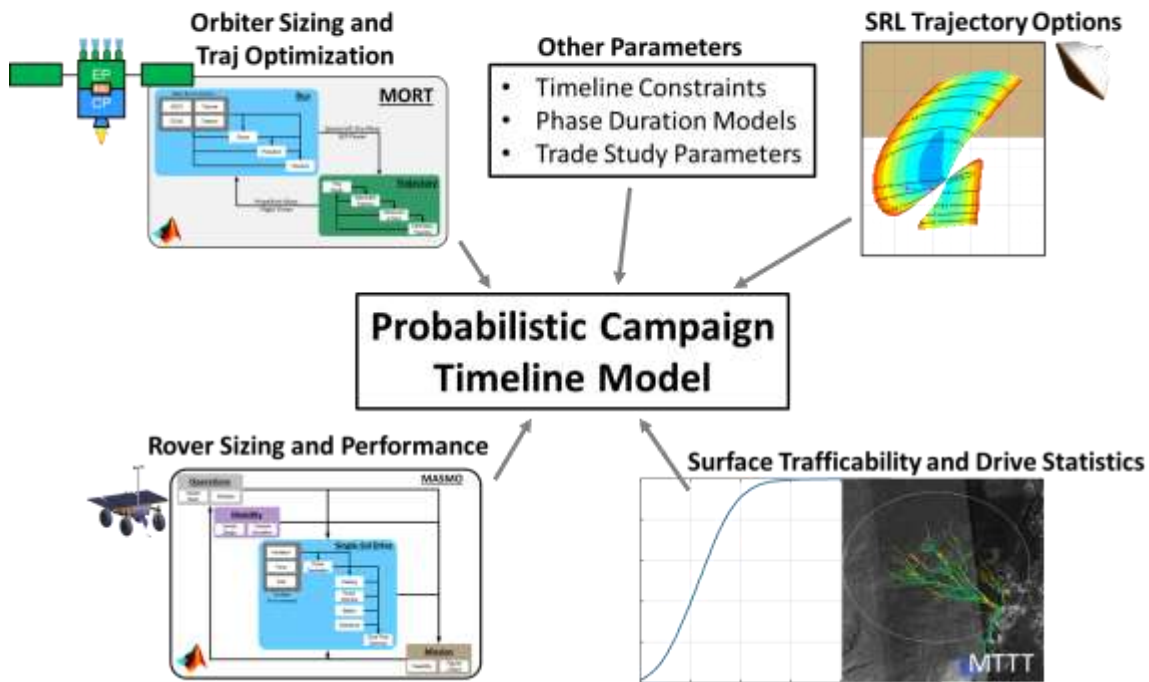


Figure 7. Tools used for campaign-level optimization

The overall analysis approach has the following steps for each set of user-specified inputs:

1. Use MORT to find the optimal spacecraft configuration for each ERO LMO arrival and departure date pair subject to launch and arrival date constraints. In this case, “optimal” means that for a given propulsion technology, the number of engines and power level/drag flap sizing is chosen to maximize launch vehicle margin. This results in a map of feasible date pairs for LMO arrival and departure. Dates are gridded at 1 month intervals, power at 2 kW intervals, and drag flap sizes at 2 m² intervals. The ERO spacecraft model was coordinated with ESA to ensure representativeness.
2. Use the probabilistic timeline tool to find the probability of readiness for departure for each ERO LMO arrival and departure date pair. The ERO arrival date is relevant because the MAV launch is assumed to happen only after the ERO is on station.
3. Pairs which have feasible MORT results **and** sufficiently high probability of readiness for departure are deemed feasible. Interesting cases are surfaced for examination by humans.

This process is repeated for each architecture, propulsion technology, payload mass, entry velocity, etc, to fully enumerate the option space. In the course of the campaign architecting process, over 100 million campaign option combinations were considered. Due to the inherent speed of MORT and PCTM, it is possible to brute force this fully enumerated tradespace in around a week of computation on a single workstation. This approach allows full confidence that all possible good solutions are found. Interestingly, the bottleneck is not computing the results but parsing the data and applying human interpretation to derive conclusions.

Table 3. Summary of selected ERO propulsion architectures and payload/return speed options for 26/26/29. The columns denote the propulsive architectures and propulsion technologies. The rows denote the payload options. The first row tier indicates different options of payload mass and the second tier are inertial Earth entry velocity. Each box shows the number of date and propulsion combinations that have a sufficiently high probability of readiness for the 2029 return window. A single number corresponds to one power level, one set of dates, one number of active engines. Low numbers (white background) indicate brittle architectures. N/A (red background) indicates there are no feasible options in that family.

	EP-EP			Hb-EP			Hb-Hb			Hb-CP			CP-CP
	T6	RIT	PPS	T6	RIT	PPS	T6	RIT	PPS	T6	RIT	PPS	
300 kg Payload													
11.2 km/s	N/A	348	N/A	865	1176	54	691	1233	N/A	N/A	N/A	N/A	N/A
11.5 km/s	217	654	N/A	1195	1765	541	1365	2093	376	N/A	N/A	N/A	N/A
12.0 km/s	352	834	251	1512	2062	868	1924	2791	717	636	1011	N/A	975
13.0 km/s	487	1181	466	2015	2646	1322	2870	3879	1162	1243	1833	339	1327
14.0 km/s	632	1413	713	2176	3038	1705	3520	4662	1390	1518	2202	396	1537
400 kg Payload													
11.2 km/s	N/A	172	N/A	620	882	N/A	284	589	N/A	N/A	N/A	N/A	N/A
11.5 km/s	82	408	N/A	914	1356	182	640	1264	N/A	N/A	N/A	N/A	N/A
12.0 km/s	171	494	96	1225	1651	364	1012	1748	187	N/A	403	N/A	573
13.0 km/s	284	764	248	1631	2188	668	1643	2653	380	495	883	N/A	773
14.0 km/s	336	984	330	1792	2568	818	2189	3332	494	610	1046	N/A	775
500 kg Payload													
11.2 km/s	N/A	N/A	N/A	382	589	N/A	N/A	N/A	N/A	N/A	N/A	N/A	N/A
11.5 km/s	N/A	218	N/A	653	977	N/A	257	612	N/A	N/A	N/A	N/A	N/A
12.0 km/s	N/A	313	N/A	876	1284	N/A	427	992	N/A	N/A	N/A	N/A	N/A
13.0 km/s	154	467	112	1201	1739	N/A	852	1637	N/A	N/A	N/A	N/A	N/A
14.0 km/s	203	653	143	1422	2092	286	1209	2147	N/A	N/A	271	N/A	N/A
600 kg Payload													
11.2 km/s	N/A	N/A	N/A	N/A	312	N/A	N/A	N/A	N/A	N/A	N/A	N/A	N/A
11.5 km/s	N/A	N/A	N/A	393	616	N/A	N/A	251	N/A	N/A	N/A	N/A	N/A
12.0 km/s	N/A	159	N/A	557	893	N/A	N/A	459	N/A	N/A	N/A	N/A	N/A
13.0 km/s	N/A	288	N/A	810	1268	N/A	379	897	N/A	N/A	N/A	N/A	N/A
14.0 km/s	110	403	N/A	1043	1578	N/A	596	1219	N/A	N/A	N/A	N/A	N/A

Table 3 shows some of the condensed results from the broadest search level (displaying all of them is not suitable for printed format). The results shown are from the most aggressive (lightest weight) spacecraft model considered feasible and with the most possible equipment staged after rendezvous activities. This included specifically most of the communications equipment, the reaction wheels, spent tanks and engines, and the parts of the payload not needed for EEV release. Less aggressive designs had fewer or no feasible solutions. From these results, it is possible to draw several important conclusions.

- There are valid architectural options for every propulsion architecture and engine type, but some are more robust than others.
- Among the hybrid options, Hb-EP is clearly the dominant architecture (significantly more robust than Hb-Hb and Hb-CP for a given payload/engine). Hb-EP also has the advantage of not having a TEI critical event and associated orbit plane constraints.
- CP-CP does not have any valid options for the heavier payloads (500 kg or higher).
- Within a given propulsion family, the PPS thruster is inferior to the other options for this application (has fewer valid architectures for a given architecture/payload).
- RIT and T6 options are generally similar, with RIT having the slight edge.
- The 14 km/s entry speed is not strongly beneficial. This can be seen by comparing the 13 km/s row and the 14 km/s row for a given payload/propulsion combination. There are very few options enabled by the 14 km/s line, though it does offer robustness.

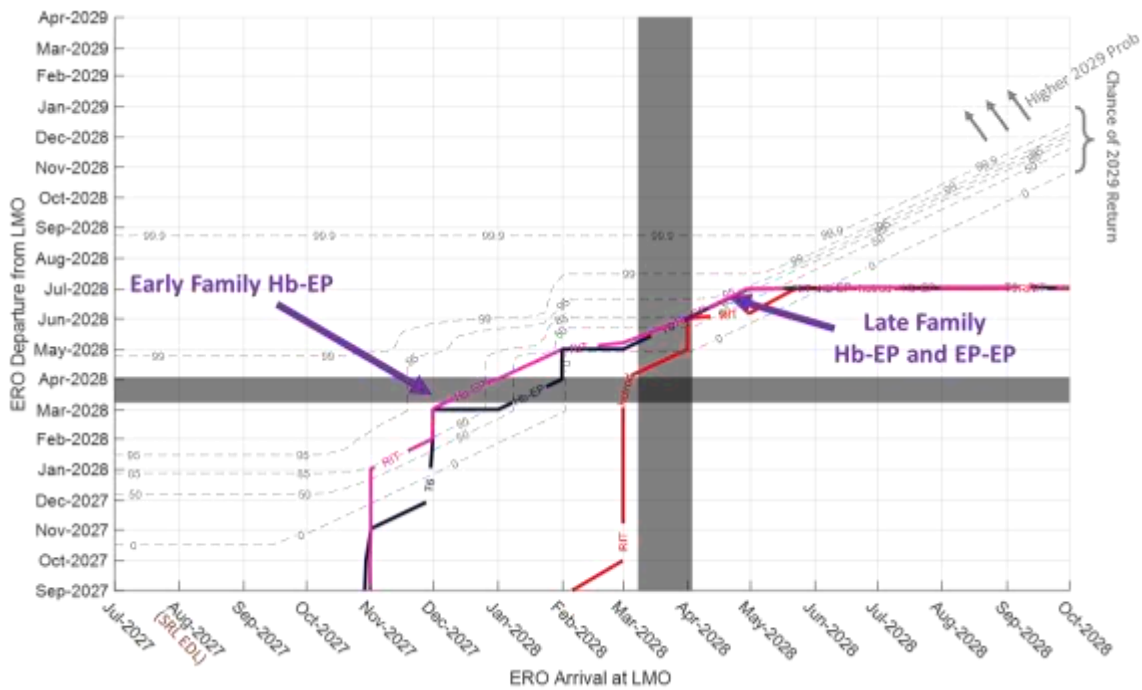


Figure 8. Timeline and ERO trajectory feasibility map for select cases (500 kg payload at 13km/s). The three contours shown (red: EP-EP RIT, magenta: Hb-EP RIT, black: Hb-EP T6) are the three feasible families. All date pairs below and to the right of the contours are feasible in timeline and launch margin. The dashed grey contours represent the probabilistic timeline figure of merit. It is important to note that the timeline figure of merit is not the actually expected chance but rather an indicator of architectural difficulty based on current models. The gray boxes are solar conjunction (same date ranges on both axes). Two distinct feasible families arise as optimal and are noted.

To examine these solutions further, additional analysis was done for the 500 kg payload at 13.0 km/s entry speed. This is considered the “nominal” payload at the present time in the study. Figure 8 shows the timeline and ERO trajectory feasibility maps. Two distinct families arise as optimal: the “early” family (applies only to Hb-EP) arrives and departs prior to solar conjunction and the “late” family arrives and departs after solar conjunction.

The early family is a more CP-like hybrid characterized by a very large outbound CP maneuver, putting the ERO almost all the way into LMO immediately after MOI and with lower power and fewer engines but more time to complete the return leg. The MAV launch is limited by surface mission speed and would launch as soon as the MAV is ready, in Dec 2027 or Jan 2028 and rendezvous activities would be complete by March 2028 to begin spiral up.

The late family is a more EP-like hybrid characterized by a smaller (but still large) outbound CP maneuver, but still with some significant spiraling such that arrival to LMO is not until May 2028. The MAV launch would be awaiting the ERO and would occur shortly after the ERO reaches LMO. Rendezvous would need to be completed quickly in time for a July 2028 LMO departure. There are also even higher power EP-EP options that fall into a similar family.

Having used the big data approach to broadly search the space, the most favorable five options were studied in further detail and locally optimized by humans, which improved upon the automated solutions modestly. In all cases, there is positive launch vehicle margin, and the spacecraft sizing model predicts that a feasible spacecraft meeting the propulsion, power, and propellant needs can be constructed. These cases and some figures of merit are shown in Table 4.

Table 4. Summary of top five ERO families from 26/26/29 architecture exploration for 500 kg payload and 13.0 km/s Earth entry speed constraint. All cases have 3 months in LMO. The EP-EP cases do a heliocentric rendezvous with Mars and start the circular spiral from the sphere of influence (SOI). The Hb-EP cases have a starting periapsis around 500 km and a starting apoapsis as listed.

Case	Propulsion			Launch Configuration				Return Stage		Trajectory Info							
	Type	Active Thrusters	Power [kW]	Wet Mass	Dry Mass	Xenon Mass	Chem Mass	Dry Mass	Xenon Mass	Earth Launch	Launch C3	Mars Arrival V_{∞}	Spiral Start Apoapsis	LMO Arrive	LMO Depart	Earth Arrival	Min Hel Dist [AU]
1	EP-EP	RITx7	77	6196	3633	2475	0	2551	812	Jun-2026	4.1	≈ 0	(SOI)	Mar-2028	Jun-2028	Nov-2029	0.82
2	Hb-EP	T6x3	30	5865	2720	622	2467	1432	281	Oct-2026	6.4	2.0 km/s	1,350 km	Nov-2027	Mar-2028	Sep-2029	0.92
3	Hb-EP	T6x4	47	6092	3087	848	2092	1792	307	Oct-2026	5.0	1.5 km/s	2,200 km	Jan-2028	Mar-2028	Aug-2029	0.98
4	Hb-EP	RITx3	33	5886	2761	683	2384	1511	287	Oct-2026	6.3	1.9 km/s	1,235 km	Nov-2027	Mar-2028	Sep-2029	0.87
5	Hb-EP	RITx4	58	5776	3110	1464	1130	1962	639	Oct-2026	7.1	1.4 km/s	13,000 km	Mar-2028	Jun-2028	Nov-2029	0.83
14	Hb-EP	RITx3	33	5995	3243	1262	1269	2691	1262	Oct-2026	5.6	2.1 km/s	33,000 km	Dec-2028	Aug-2029	Oct-2031	0.97

It is particularly interesting to compare cases 4 and 5. In both cases, the Hb-EP architecture with RIT engine technology is utilized, and both have 3 months in LMO. However, the spacecraft sizing and trajectory choices are quite different. As compared to the EP-like case #5, the CP-like case #4 has much lower power, much lower xenon load, and much higher CP load, by a factor of roughly two in each case. It also arrives much earlier (Nov 2027 vs Mar 2028) by inserting chemically into a very low apoapsis (1,235 km vs 13,000 km), and has to do very little EP thrusting to reach LMO. Case #4 departs earlier (March vs June 2028) and takes a longer return trajectory due to the lower acceleration. The case #5 return trajectory is significantly less efficient, needing to fly closer to the sun and arriving later than optimal. However, because of the higher acceleration, this is possible. The increased inbound propellant load is offset by the significantly more efficient outbound trajectory, requiring much less CP than case #4 due to the lower Mars arrival velocity and higher starting apoapsis. Finding these two different families showcases the power of the exhaustive approach – it would have been impossible to predict these particular combinations of engines, power, orbits, etc a priori. Further, utilizing the spacecraft from case #4 on the case #5 trajectory or vice-versa would be infeasible. This highlights the importance of optimizing the spacecraft and trajectory design simultaneously.

Overall, the early family Hb-EP (cases 2 and 4) seem to be the most promising because of the significantly lower power level needed and the ability to launch the MAV in late 2027, corresponding with L_s values between 180 and 225. The late-family cases need to launch the MAV in April 2028, which corresponds with $L_s \approx 290$, which is nearly the coldest and least sunny time at the MSR landing site. It also requires the surface mission to survive longer on the surface, and in the time period after $L_s = 180$, there is a risk of global dust storms. Therefore, less time on the surface is better. Launching the MAV without the ERO on-station could be considered to avoid these issues, but it is then not clear that the ERO could complete rendezvous activities in time because the search for the OS might take significantly longer. More detailed trajectory and timeline plots for case #4 are shown in Figure 9 and Figure 10. This type of information is available for all of the millions of cases, but is this one case is displayed as an example.

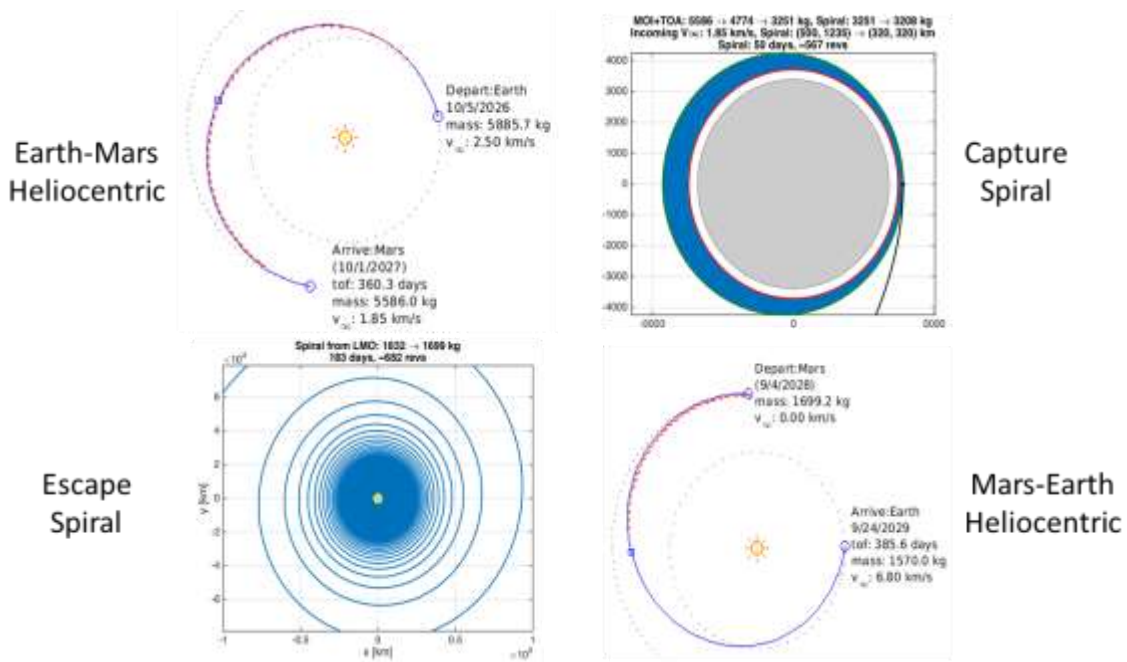


Figure 9. Trajectory plots for case #4 (26/26/29) showing the four primary propulsive maneuvers

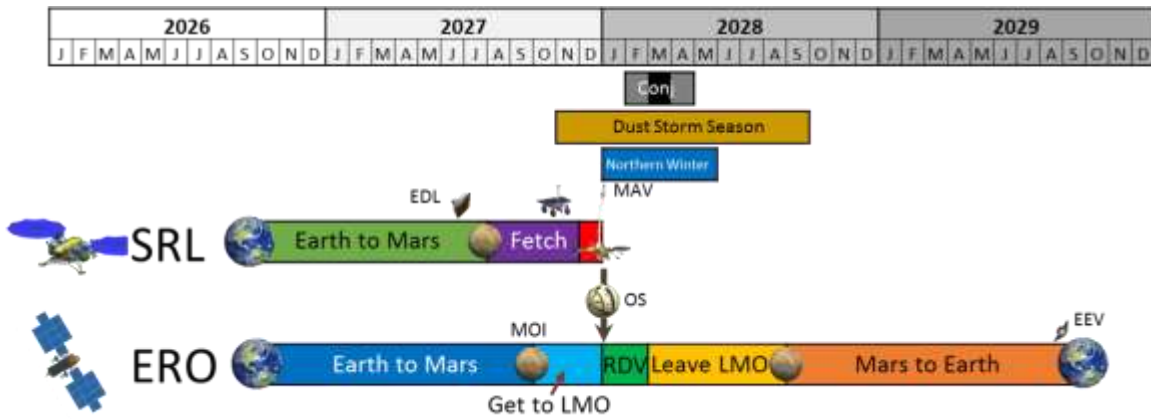


Figure 10. Timeline summary for case #4 (26/26/29)

Observations

Based on the overall 26/26/29 results, several observations can be made:

- The Hb-EP ERO propulsive architecture is the best overall EP-involving architecture, in combination with the RIT or T6 engines. For larger payload masses, it is the best propulsive architecture overall.
- The CP-CP architecture struggles with launch vehicle feasibility for larger payload masses (500 kg and above) but would be feasible (and perhaps preferred) for lower payload masses or improved launch vehicle performance.

- In all cases, the lightest possible ERO with the maximum staging will be needed to meet the launch vehicle and return constraints.
- The surface mission would likely land around $L_s=135$ and the MAV would likely launch no earlier than $L_s=205$ and potentially as late as $L_s=300$. This means that SRL and SFR may both need to operate in the historically observed global dust storm season as well as the northern winter, which could result in consideration of radioisotope power systems for power or thermal control.
- For the early-family architectures (which seem to be most favorable) the surface mission will be under time pressure to be ready for MAV launch. This will lead to very high traverse speed needed from SFR and autonomy in SFR and SRL. This may incentivize improved landing precision from SRL (including pinpoint landing).
- It is not feasible for ERO to be on-station to provide relay support for SRL or the early part of the surface mission. This would need to be provided by an existing or new asset. However, it is feasible and reasonable for ERO to support MAV launch (and is actually desirable from a timeline perspective).

26 / 26 / 31 CAMPAIGN OPTION

The next option considered is a five-year option with SRL and ERO launching in 2026 and the ERO returning in 2031. The additional two years of time allows a wider variety of trajectory options for both SRL and ERO to be considered. A similarly exhaustive analytical process was followed as for 26 / 26 / 29 in enumerating all options, finding the most interesting families, and examining those in further detail. In the interest of brevity, the intermediate steps have been largely omitted and the interesting differences and results are shown in this section.

SRL Trajectory Options

With the longer timeline, it is possible to consider a wider variety of SRL trajectory options than the typical half-revolution solutions employed by all previous Mars missions to-date. In particular, the 1½-revolution solutions (“type III/IV”) solutions are available. Figure 11 shows an extended porkchop plot showing these solutions alongside the half-rev solutions considered previously. Due to TRN needing to be able to image the ground for landing safety, landing dates in the likely dust storm season are not desirable. In the remaining areas, there are two families additional families with reasonably low C3, entry velocity, and high enough lighting angles. The first (“A”) arrives around $L_s=0$, just after the end of the dust storm season and is characterized by extremely low entry velocity. The second (“B”) arrives around $L_s=100$ to 120, exact value depending on the mass and launch vehicle performance (better performance allows earlier landing and lower entry velocity). The 26/26/29 opportunity is also still valid for 26/26/31.

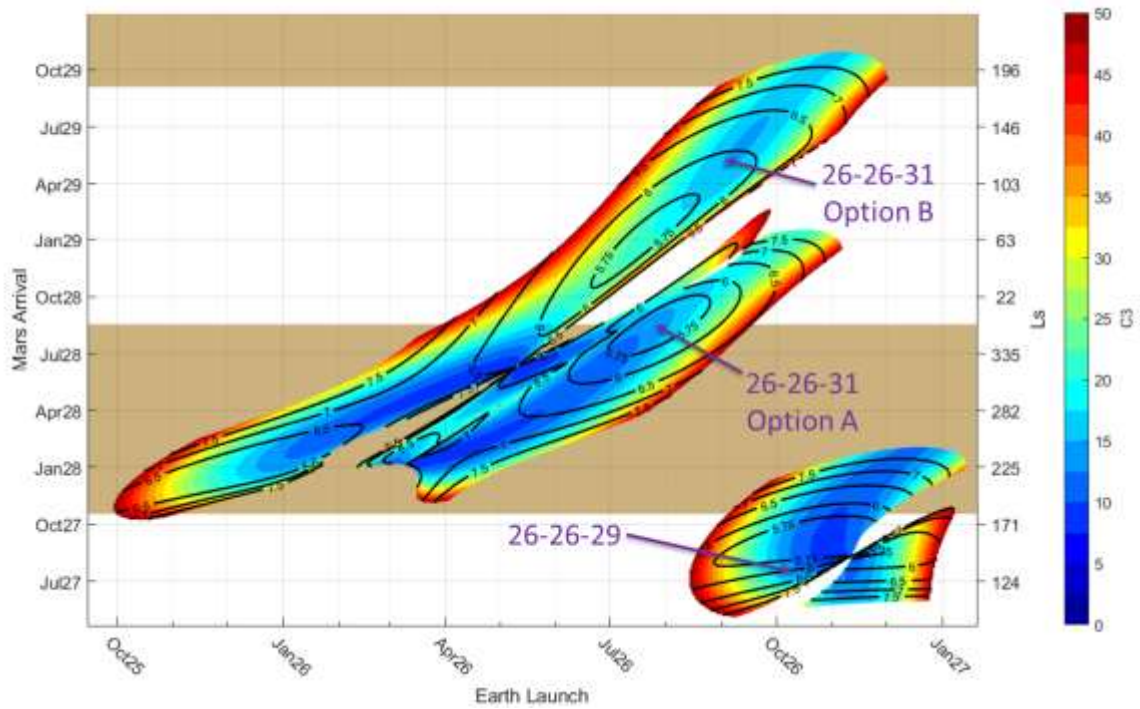


Figure 11. SRL launch/arrival options (“porkchop plot”) for 26/26/31. Colored contours are launch energy (C3) in km^2/s^2 , solid black contours are inertial entry speed, in km/s . The tan region corresponds to $L_s=180$ to 360 and denotes the time when global dust storms are most likely.

All three of these opportunities were considered fully (including impacts on the ERO trajectory and surface mission), but Option A was architecturally dominant in every case. This arises from three primary reasons:

- For a surface mission starting around $L_s \approx 0$, the entire surface mission can occur well before the onset of the historically observed dust storm season starting at $L_s \approx 180$
- The ERO benefits more from an earlier departure than a later arrival (arrival to support $L_s \approx 0$ SRL EDL is already sufficiently late).
- Landing at $L_s \approx 0$ is better from an EDL perspective due to the increased atmospheric density

A more zoomed in porkchop plot in the area of Option A is shown in Figure 12 including an example launch period. Again, this is representative and small changes in this region are expected. This particular launch period was straightforwardly the lowest entry velocity, lowest C3, highest solar elevation angle, and earliest option after the $L_s \approx 0$ cutoff for dust storm season.

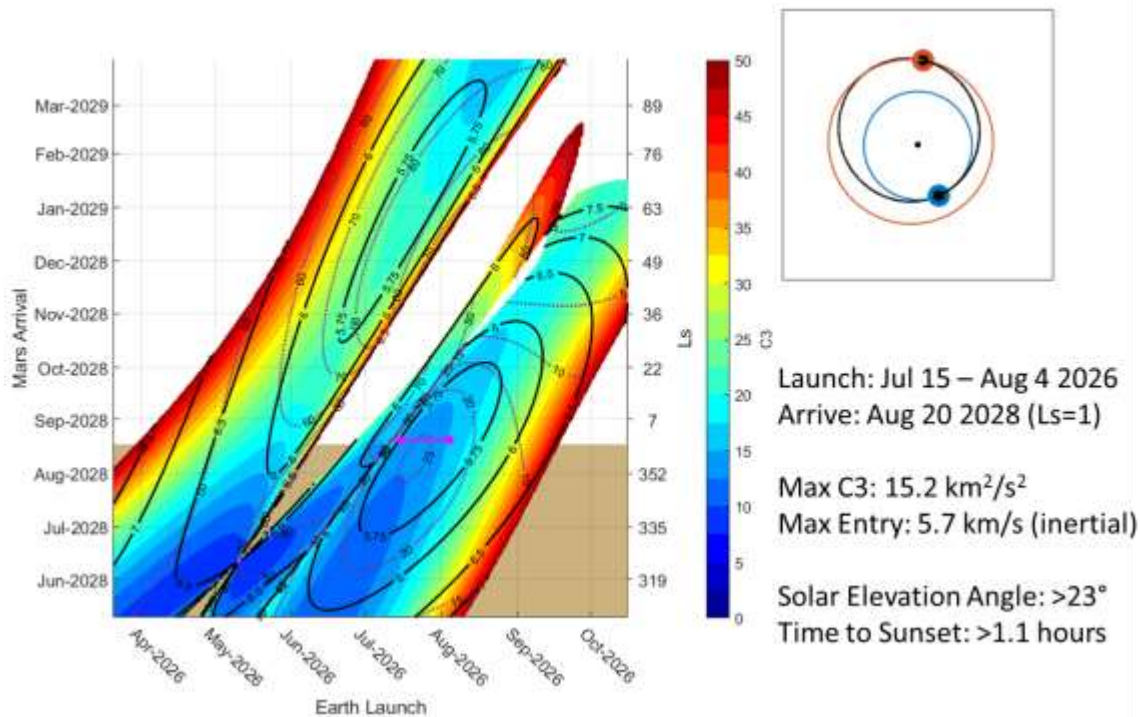


Figure 12. SRL launch/arrival options (“porkchop plot”) for 26/26/31 Option A. Colored contours are launch energy (C_3) in km^2/s^2 , solid black contours are inertial entry speed, in km/s , dotted purple contours are the solar elevation angle at landing, in degrees. The tan region corresponds to $L_s=180$ to 360 and denotes the time when global dust storms are most likely. The magenta line is the selected launch period. An illustration of the trajectory and some figures of merit are shown on the right.

ERO Trajectory Options

Like the SRL, the additional time opens up significantly more trajectory options for ERO. Figure 13 show the outbound launch and LMO arrival performance for a sweep of dates. This plot is similar to Figure 3, but with later arrival options shown. From these plots, one of the most important conclusions can be readily shown – the extra time is immensely beneficial to EP-involving options and only slightly beneficial to CP options due to the increased aerobraking time. Further, the CP options derive almost no benefit at all on the return leg while the EP options also make substantial improvements either by taking more efficient transfers or enabling reduced accelerations. As a result, the EP-involving options were capable of adding much more flexibility to the campaign and were prioritized for further study. Similarly (and for the same reasons as in 26/26/29), the Hb-Hb and Hb-CP architectures were once again inferior to the Hb-EP architecture and were discarded early as well. Though there were feasible PPS options in many cases, due to the much lower I_{sp} , they are significantly inferior to the gridded ion options in all cases. From an architectural perspective, the difference between RIT and T6 is minimal, and will not be addressed further here. RIT is assumed going forward for simplicity.

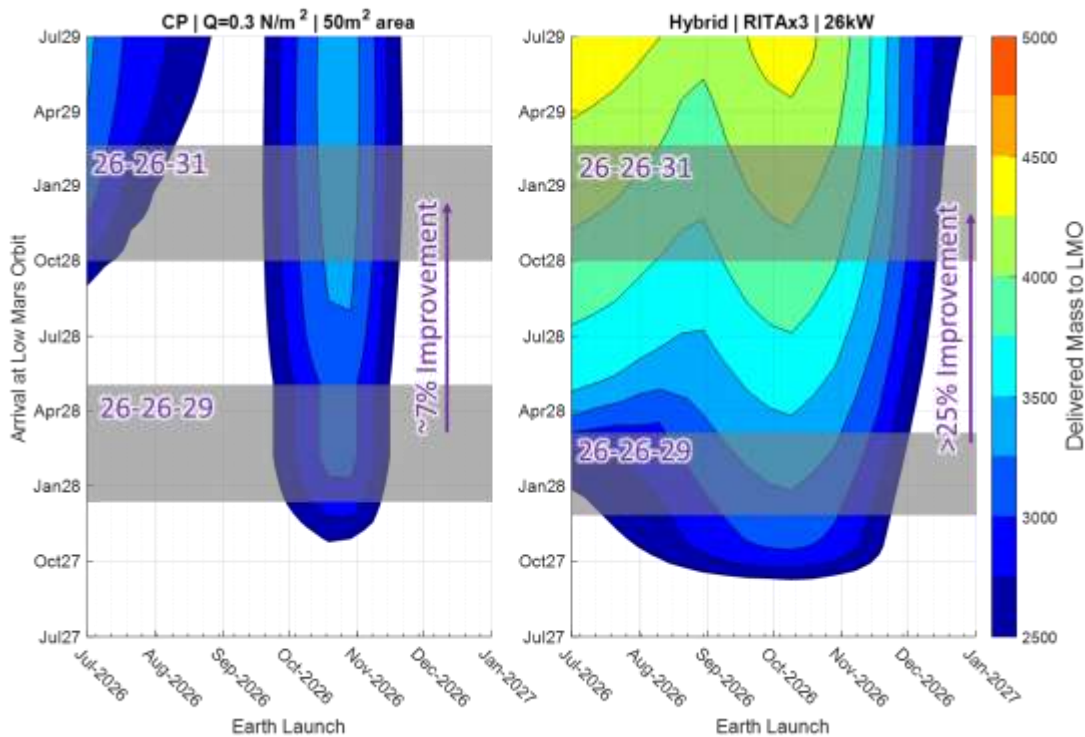


Figure 13. Example Outbound ERO transfer options for 26/26/31 option. Left: CP with aerobraking, Right: Hybrid. Approximate LMO arrival dates consistent with return are shown in the gray boxes. Exact arrival date needed in these ranges depends on return trajectory and rendezvous strategy. These plots include a 21 day launch period in each point.

The remaining architectures are then the EP-EP and Hb-EP. An exhaustive search over various payload, staging, and spacecraft subsystem sizing options was performed, but is omitted for brevity. Both architectures present the ability to be significantly less aggressive than the assumptions used for the 26/26/29 options, but the Hb-EP option was dominant for the following reasons:

- Using a CP stage allows more flexibility in arriving earlier to meet SRL EDL needs. In particular, it allows full utilization of the launch vehicle mass capability. The EP-EP option is frequently unable to maximize use of the launch vehicle because it is acceleration-limited on the outbound heliocentric leg. Arriving and departing later (e.g. by moving to SRL Option B) does not improve the EP-EP situation, as this then trades acceleration limits on one leg for the other.
- Hb-EP options overall need lower power and tolerate heavier arrays that are more consistent with existing solar array technology used on communications satellites. EP-EP options need more power and benefit strongly from lightweight arrays.
- Using a CP stage allows a simpler EP system which can be hosted entirely on the return stage, alleviating the need to jettison or stage any EP equipment. The EP-EP options all require staging some EP equipment.

Table 5, Figure 14, and Figure 15 show an example 26 / 26 / 31 option using RIT engines, a 500 kg payload and an entry velocity constraint of 12.0 km/s. Staging and spacecraft mass esti-

mates are less aggressive than used for 26/26/29, meaning that that dry mass values (especially the dry mass of the return stage) are noticeably higher.

Table 5. Summary of dominant ERO family from 26/26/31 architecture exploration for 500 kg payload and 12.0 km/s Earth entry speed constraint.

Case	Propulsion			Launch Configuration				Return Stage		Trajectory Info							
	Type	Active Thrusters	Power [kW]	Wet Mass	Dry Mass	Xenon Mass	Chem Mass	Dry Mass	Xenon Mass	Earth Launch	Launch C3	Mars Arrival V ∞	Spiral Start Apoapsis	LMO Arrive	LMO Depart	Earth Arrival	Min Hel Dist [AU]
14	Hb-EP	RITx3	33	5995	3243	1262	1269	2691	1262	Oct-2026	5.6	2.1 km/s	33,000 km	Dec-2028	Aug-2029	Oct-2031	0.97

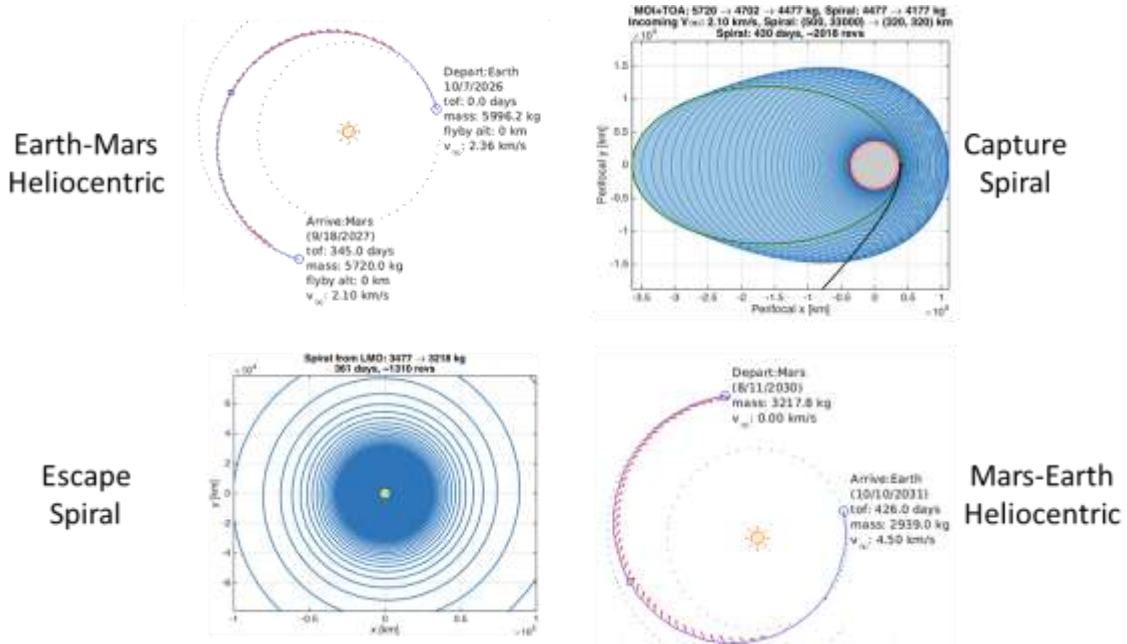


Figure 14. Trajectory plots for case #14 showing the four primary propulsive maneuvers

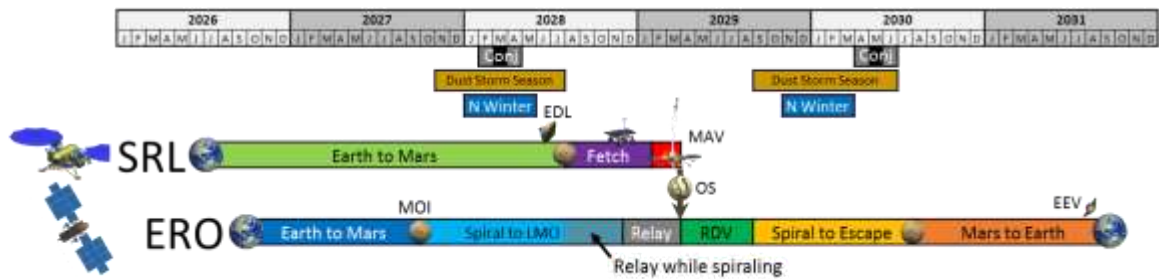


Figure 15. Timeline summary for 26/26/31 option case #14

Comparison to 26 / 26 / 29

This section contains a technical comparison between the 26/26/29 (3-year) and 26/26/31 (5-year) options described so far. A timeline comparison is shown in Figure 16.

From a trajectory perspective, the MOI for both options is at roughly the same time and speed. The biggest difference is that the 26/26/31 option can spend significantly more time spiraling and as a result can start at higher altitude. This saves significant propellant by doing the altitude reduction with EP instead of CP. The 26/26/31 option can also support significantly more mass, especially on the return leg. The return leg is qualitatively similar, but takes much longer due to the significantly reduced acceleration and lowered hyperbolic velocity at Earth. This has benefits in reducing the staging aggressiveness and allowing a heavier spacecraft (which reduces development risk). The 26/26/31 option can also support a lower Earth entry speed and indeed benefits less from the higher speeds utilized in the 26/26/29 option due to the reduced accelerations. This also has the effect of increasing the minimum solar distance to ~1 AU.

In 26/26/31, the ERO can be present for the entire SRL surface mission. This is infeasible for 26/26/29 due to how early the SRL needs to arrive in order to complete its mission in time to support the return window. This alleviates reliance on other relay assets. A significantly longer surface mission (8+ months instead of ~5 months) and rendezvous time (~5 months instead of ~3 months) is enabled. The increased rendezvous time may enable larger MAV dispersions and/or a more propellant efficient orbit matching strategy.

Further, the 26/26/31 case entirely avoids the historically-observed dust storm season and the entire surface mission occurs in northern spring/summer, an energetically favorable season for SRL and SFR. Both of these effects reduce the possibility that radioisotope material would be needed. There are likely benefits for other SRL and SFR subsystems (e.g. by reducing solar array size).

Although the 26/26/31 option encounters two solar conjunctions, they both occur when the missions are doing routine in-space maneuvering (SRL: heliocentric cruise, ERO: high altitude spiraling). In 26/26/29, the conjunction occurs just after the rendezvous and during payload operations. This increases risk, especially in contingency scenarios, potentially leading to a need for even faster rendezvous operations to avoid it.

While there are few technical downsides to the 26/26/31 option, it would entail an earlier launch of SRL (in July 2026 instead of October) and return of the samples to Earth 2 years later.

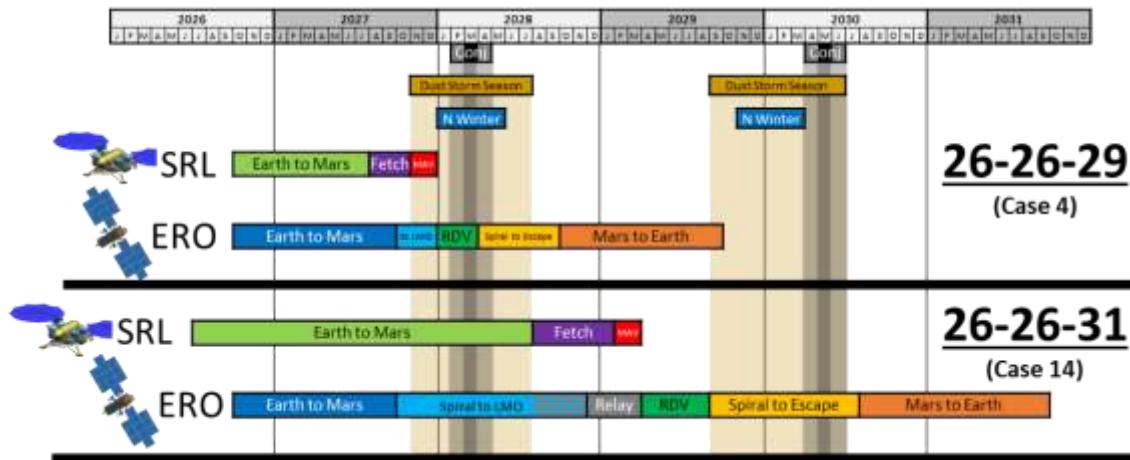


Figure 16. Timeline comparison between 26/26/29 and 26/26/31 cases

OTHER CAMPAIGN OPTIONS

The 26/26/29 and 26/26/31 options were described in significant detail in this paper. For brevity, the other options were not detailed as thoroughly, though they have been investigated in significant level of detail during this study. Below is a summary of these options:

28/28/31 – The 28/28/31 campaign option is broadly similar to 26/26/29, but one synodic period later. Relative to the Mars seasons, there is a shift of around 2 months later due to the Earth-Mars geometry. The main effect of this is to push the surface mission even further into the cold and dusty seasons, making it more challenging than 26/26/29. This would increase the need for long diverts and could result in consideration of using radioisotope material to counter the environmental difficulties. For CP ERO options, the Earth-Mars transfer is slightly worse due to increased C3 and Mars arrival velocity, but these can be more-than-offset by using an Earth flyby and a 2027 launch. The CP return transfer in 2031 is very slightly better than the 2029 one. For EP-involving transfers, there is not much difference between the opportunities. Due to the use of the Earth flyby, the CP-CP architecture is on equal footing with Hb-EP options in this opportunity in terms of trajectory feasibility.

28/28/33 – The 28/28/33 campaign option is broadly similar to 26/26/31, but one synodic period later. A significant difference is that the SRL Option A transfer arriving at $L_s \approx 0$ has a much higher C3 requirement for a ballistic transfer in 2028. There are three options for resolving this: use a larger launch vehicle (Falcon Heavy has the capability), modestly increase the in-space propulsive capability of the cruise stage (either CP or EP), or take the Option B transfer, which is available in 2028. If an $L_s \approx 0$ SRL arrival is to be maintained, the ERO has a slightly higher CP maneuver to be in position to start relay, but this is more than offset with the use of a 2027 launch combined with an Earth flyby. The ERO LMO departure date is relaxed by around 2 months.

26/28/31 – To first order, the SRL would be similar to 26/26/31 while the ERO would be similar to 28/28/31. The ERO would not be able to provide relay support for the SRL surface mission. There would be a choice between designing the SRL to survive until ERO is ready for MAV launch (which would be into the dust storm season) or having the ERO find the OS at a later time.

28/26/31 – To first order, the SRL would look like 28/28/31. This has the effect of launching the MAV substantially later than 26/26/31, meaning the ERO would need to have a faster return leg than the ERO of 26/26/31. This would either entail higher acceleration Hb-EP (less mass, more jettison, or more power), or a Hb-Hb to augment the return leg with some CP.

26/26/33 – Overall, the only benefit here beyond 26/26/31 is extra time for the ERO return leg. This may slightly reduce the power or propellant needs and offer slightly more surface time, but the effect is minimal.

26/28/33 – It is not clear that this actually has any benefit over 28/28/33, as it would require either having the SRL survive a full Martian year (including winter and dust storm season), or launch the MAV >1 year before the ERO would arrive. Delaying the SRL launch to 2028 is likely preferable if the ERO cannot launch until 2028 and Earth return is in 2033.

28/26/33 – This option would allow the ERO additional time to get to LMO ahead of SRL and take a more propellant-efficient transfer. However, the 28/28/33 option is already fairly efficient and already fits in the constraints (and may launch in 2027 anyway), so the benefit here is minimal. EP-EP options benefit more from the increased outbound transfer time and are roughly on-par with Hb-EP options in this case.

CONCLUSIONS

Campaign transportation architectures for MSR in the 2020's were exhaustively examined using a variety of trajectory and spacecraft performance modeling tools developed at JPL and in collaboration with ESA. In this paper, results were focused on the options where both ERO and SRL would launch in 2026, with returns in either 2029 or 2031. Other options were briefly mentioned by analogy though they were also analyzed in detail.

From the millions of runs, a number of favorable architectures were identified, satisfying the relevant constraints and optimizing for mission success while minimizing implementation challenge. This work highlights the importance of simultaneous spacecraft and trajectory optimization as well as thorough global campaign exploration and optimization – it is unlikely that more traditional methods of iterating on a few point designs would have found the campaign-optimal solutions uncovered by our methods.

ACKNOWLEDGMENTS

This research was carried out at the Jet Propulsion Laboratory, California Institute of Technology, under a contract with the National Aeronautics and Space Administration. The information presented about potential Mars Sample Return is pre-decisional and is provided for planning and discussion purposes only.

REFERENCES

- ¹ T. Zurbuchen (NASA), D. Parker (ESA) signatories, “Joint Statement of Intent between the National Aeronautics and Space Administration and the European Space Agency on Mars Sample Return,” 2018 Berlin Airshow, 26 April 2018.
- ² A. Karp, F. Beyer, B. Muirhead, “Mars Sample Return Lander Mission Concept,” 69th International Astronautical Congress, Bremen, Germany, 2018.
- ³ A. G. McSweeney, S. Vijendran, J. Huesing, R. E. Lock, A. K. Nicholas, “The Earth Return Orbiter Mission as part of an international Mars Sample Return Campaign.” 69th International Astronautical Congress, Bremen, Germany, 2018.
- ⁴ R.C. Woolley, F. Laipert, A.K. Nicholas, and Z.P. Olikara, “Low-Thrust Trajectory Bacon Plots for Mars Mission Design,” AAS Astrodynamics Specialist Conference. Maui, HI, Jan. 2019.
- ⁵ F. Laipert, A.K. Nicholas, Z.P. Olikara, R.C. Woolley, and R.E. Lock, “Hybrid Chemical-Electric Trajectories for a Mars Sample Return Orbiter,” AAS Astrodynamics Specialist Conference. Maui, HI, Jan. 2019.
- ⁶ R. J. Haw, E.D. Gustafson, “Mars Sample Return Orbital Rendezvous Detection Methods,” AAS Astrodynamics Specialist Conference. Maui, HI, Jan. 2019.
- ⁷ Z.P. Olikara and A.K. Nicholas, “Chemical and SEP Orbit Matching for Mars Sample Rendezvous,” AAS Astrodynamics Specialist Conference. Maui, HI, Jan. 2019.
- ⁸ A.K. Nicholas, R.C. Woolley, A. Didion, F. Laipert, Z.P. Olikara, R. Webb, and R.E. Lock, “Simultaneous Optimization of Spacecraft and Trajectory Design for Interplanetary Mission Utilizing Solar Electric Propulsion,” AAS Astrodynamics Specialist Conference. Maui, HI, Jan. 2019.
- ⁹ R.E. Lock, A.K. Nicholas, S. Vijendran, R.C. Woolley, A. Didion, F. Laipert, Z. Olikara, “Potential Campaign Architectures and Mission Design Challenges for Near Term International Mars Sample Return Mission Concepts,” AAS Astrodynamics Specialist Conference. Maui, HI, Jan. 2019.
- ¹⁰ C. D. Edwards, Jr., A. H. Farrington, R. E. Gladden, C. H. Lee, R. E. Lock, B. K. Muirhead, A. K. Nicholas, R. C. Woolley, “Proximity Link Telecommunication and Tracking Scenarios for a Potential Mars Sample Return Campaign,” 2019 IEEE Aerospace Conference. Big Sky MT, 2019

¹¹ A.M. Didion, A.K. Nicholas, J.E. Riedel, R.J. Haw and R.C. Woolley, “Methods of passive optical detection and relative navigation for rendezvous with a non-cooperative object at Mars,” AAS/AIAA Astrodynamics Specialist Conference. Aug. 2018, AAS 18-288.

¹² M. Ono, et al., “Data-Driven Surface Traversability Analysis for Mars 2020 Landing Site Selection” IEEE Aerospace Conference, 2016.

¹³ M. Ono, et al., “Mars 2020 Surface Mission Performance Analysis: Part 2. Surface Traversability,” AIAA SPACE Forum, Orlando, FL, Sept. 2018.